Rare Met. (2022) 41(5):1697–1702
DOI 10.1007/s12598-015-0554-x

RARE METALS
www.editorialmanager.com/rmet

Recovery of rare earth elements from permanent magnet scraps by pyrometallurgical process

Yu-Yang Bian, Shu-Qiang Guo*, Yu-Ling Xu, Kai Tang, Xiong-Gang Lu, Wei-Zhong Ding

Received: 23 June 2014 / Revised: 21 August 2014 / Accepted: 23 June 2015 / Published online: 17 July 2015

Abstract In order to recover valuable rare earth elements from Nd–Fe–B permanent magnet scraps, a high-temperature pyrometallurgical process was developed in this work. The magnet scraps were first pulverized and oxidized at 1000 °C in normal atmosphere. The oxidized mixtures were then selectively reduced by carbon in the temperature range of 1400–1550 °C. In this way, the rare earth elements were extracted to the form of oxides, whereas Fe and B were separated to metal phase. For improving the purity of rare earth oxides, the effects of temperature and reaction time on the reduction of B_2O_3 in oxide phase were investigated. It is found that increasing reaction temperature and extending reaction time will help the reduction of B_2O_3 contents in rare earth oxide phase. Almost all rare earth elements can be enriched in the oxide phase with the highest purity of 95 %.

Keywords Rare earth; Permanent magnet; Recycling

1 Introduction

Since the invention of sintered $Nd_2Fe_{14}B$-based permanent magnet by Sagawa et al. [1–3] in 1980s, it is widely used in many electromagnetic applications. However, about 1/4 of the alloy materials are produced as useless scraps during the manufacturing processes [4]. Under high-temperature environments, the high oxidation rate impairs magnetic properties and shortens the service life of the magnets [5–7]. It is important to find an economic way to extract rare earth elements from magnet scraps and sludge.

Several types of methods for extracting rare earth elements from magnet scraps have so far been reported in the literature. Most of the methods were based on the wet processing using commercial acid [8, 9]. A large amount of industry waste acid will thus be produced. This will unavoidably bring the environmental issues. Some of the methods introduced a new kind of metallic media to form intermediate alloys containing rare earth elements [10–13] and then separate the rare earth elements from the intermediate alloy. The way using the metallic media seems uneconomical, and these methods are not applicable to the partial oxidized magnets scrapes. The methods of selective chlorination of rare earth elements were also proposed [4, 14]. By using $FeCl_2$ or NH_4Cl as a chlorinating agent, the rare earth elements were selectively chlorinated, and the rare earth chlorides were separated from $FeCl_2$ and Fe residues by further vacuum distillation or leaching process. Based on the different affinities of rare earth elements and Fe to oxygen, a high-temperature process for extraction of the rare earth element was recently reported by Nakamoto et al. [15].

A pyrometallurgical process to recover rare earth elements from Nd–Fe–B permanent magnet was proposed in the present work. The magnet scraps were first pulverized to fine particles. The scrap powders were then fully oxidized at 1000 °C. High-temperature treatment was finally applied in order to selectively reduce Fe and B oxide impurities from mixture. The rare earth elements were successfully separated from Nd–Fe–B magnet scraps in the form of oxides.

Y.-Y. Bian, S.-Q. Guo*, Y.-L. Xu, X.-G. Lu, W.-Z. Ding
Shanghai Key Laboratory of Modern Metallurgy and Materials Processing, Shanghai University, Shanghai 200072, China
e-mail: sqguo@shu.edu.cn

K. Tang
SINTEF Materials and Chemistry, 7465 Trondheim, Norway

2 Experimental

2.1 Experimental procedures

The experimental process is illustrated in Fig. 1a. The commercial Nd–Fe–B magnets without magnetization were used as raw materials in the present work. The main compositions of the magnet are Fe, Nd, Pr, La, Al and B, and the concentration of each element is shown in Table 1. The Nd–Fe–B ingots were mechanically pulverized into fine particles and sieved to less than 150 μm to accelerate the following oxidation process. The Nd–Fe–B powder mixtures were heated up to 1000 °C in a muffle furnace under air atmosphere for 2 h. After the oxidation process, the Nd–Fe–B material converted to the mixture of the oxides, mainly containing rare earth oxide (REO), Fe_2O_3, Al_2O_3 and B_2O_3. Then, the oxides were treated in the reduction process. The production of the reduction process was REO-containing oxides slag and the iron metal phase. By the separation of slag and metal, the REO-containing oxides were finally obtained.

In the reduction procedure, the oxidized Nd–Fe–B particles were placed in graphite crucible (32 mm in inner diameter and 50 mm in height) in an electric furnace with $MoSi_2$ heating elements. Carbon powders were put on the bottom of the crucible in order to protect the graphite crucible and accelerate the rate of the reduction process. The samples were then heated up to the designed reduction temperature (1400, 1500 and 1550 °C, respectively) under Ar atmosphere for 1, 3, 5 and 7 h, respectively. The Ar flow rate was controlled at 200 $ml \cdot min^{-1}$. The samples were then cooled down to room temperature under the Ar inert atmosphere. Details of the experimental set-up are given in Fig. 1b.

Table 1 Composition of bulk NdFeB magnet (wt%)

Fe	Nd	Pr	La	B	Al
61.60	30.73	4.39	1.58	0.96	0.83

2.2 Characterizations

The NdFeB samples were analysed by differential scanning calorimetry and thermogravimetry (DSC–TG, NETZSCH STA 449F3) at the heating rate of 10 $K \cdot min^{-1}$ in the temperature range of 50–1000 °C in air. The enthalpy curves were normalized to 1 mg. Calibration was achieved using Al_2O_3 as the reference material. The oxidation products at different temperatures were characterized by X-ray diffraction (XRD, D/MAX2200 V, Rigaku) using a Cu-Kα radiation with the scanning speed of 8 $K \cdot min^{-1}$.

The microstructures of the high-temperature reduced samples were examined using the backscattered-electron scanning electron microscopy (BSE–SEM, SU-1510, Hitachi) and energy-dispersive spectrometer (EDS, Oxford INCA EDS system). The REO-containing slag and metal phase were observed by optical microscopy (OM, DM 6000M, Leica). The chemical compositions of Nd, Pr, La, Fe, Al and B were analysed using inductively coupled

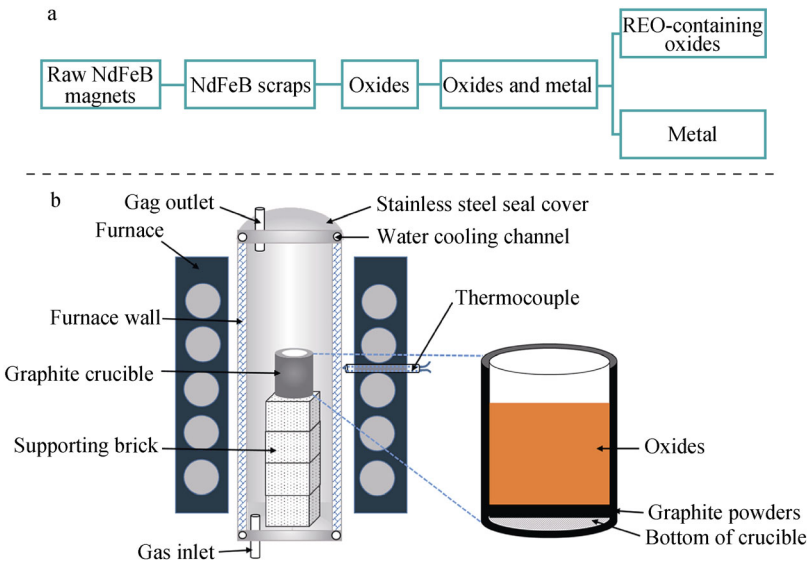

Fig. 1 Illustration of experimental process for recovery of rare earth elements from permanent magnet **a** and demonstration of apparatus used in reduction process **b**

plasma atomic emission spectrometer (ICP-AES, PE400, PerkinElmer).

3 Results and discussion

3.1 Oxidation process

The DSC–TG curves of Nd–Fe–B powders during oxidative heating process are shown in Fig. 2. In the low temperature range of 100–300 °C, the DSC curve shows a series of small exothermic reactions. In the temperature range of 350–450 °C, it shows two further exothermic peaks, marked as Peaks 1 and 2. Peak 3 is observed at around 720 °C. In order to identify the oxidation products at different temperatures, XRD analysis was performed for samples heated up to 320, 390, 700 and 1000 °C, respectively. The corresponding XRD patterns are shown in Fig. 3.

The sample before oxidation consists of three phases: $Nd_2Fe_{14}B$ matrix phase, Nd-rich boundary phase and

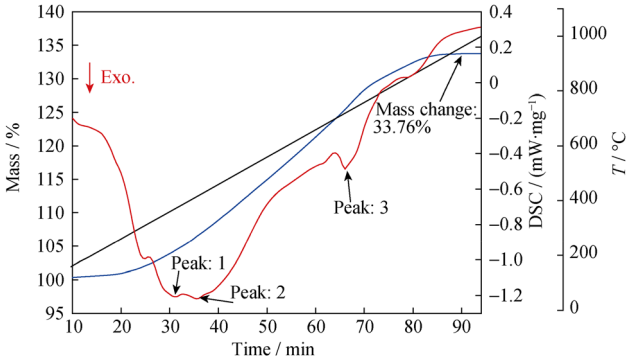

Fig. 2 DSC–TG curves of magnet powders in temperature range of 50–1000 °C under air atmosphere at heating rate of 10 °C·min^{-1}

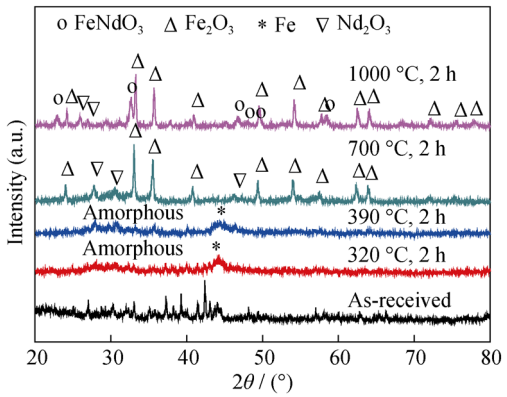

Fig. 3 XRD patterns of NdFeB samples at different oxidation temperatures for 2 h

$Nd_{1.1}Fe_4B_4$ phase [7]. $Nd_2Fe_{14}B$ Phase was identified by XRD analysis, as shown in Fig. 3. The contents of other two phases are small, and Nd-rich phase and $Nd_{1.1}Fe_4B_4$ phase are overlapped. After oxidation roasting at 320 °C for 2 h, the XRD patterns show that the main $Nd_2Fe_{14}B$ phase begins to disappear, and Fe and amorphous Nd_2O_3 phase appear. It is concluded that at the temperatures of <320 °C, the original Nd-rich phase is oxidized and part of $Nd_2Fe_{14}B$ phases are decomposed into Nd_2O_3, B_2O_3 and Fe according to Reactions (1) and (2). XRD patterns of samples at 390 °C show that $Nd_2Fe_{14}B$ phase disappears and amorphous Nd_2O_3 increases. It reveals that the further decomposition of the remaining $Nd_2Fe_{14}B$ phase is around Peak 1 in DSC curve. The difference of XRD patterns between 390 and 700 °C shows the appearance of Fe_2O_3. It can be concluded that the exothermic Peak 2 is corresponding to the formation of Fe_2O_3, represented by Reaction (3). Because B content is quite low, there is no signal of B_2O_3 found in XRD patterns. However, boron is rather easy to be oxidized, as indicated by Reaction (4). At temperature around 720 °C, an exothermic reaction occurs. From the difference of XRD patterns, it can be confirmed that Reaction (5) takes place to form $FeNdO_3$ at 720 °C [16].

$$2Nd + 3/2O_2 = Nd_2O_3, \Delta G^{\circ}(300\,^{\circ}C) = -1642\,kJ{\cdot}mol^{-1} \quad (1)$$

$$Nd_2Fe_{14}B + 9/4O_2 = Nd_2O_3 + 1/2B_2O_3 + 14Fe, \quad \Delta G^{\circ}(320\,^{\circ}C) = -2743\,kJ{\cdot}mol^{-1} \quad (2)$$

$$2Fe + 3/2O_2 = Fe_2O_3, \Delta G^{\circ}(700\,^{\circ}C) = -565\,kJ{\cdot}mol^{-1} \quad (3)$$

$$2B + 3/2O_2 = B_2O_3, \Delta G^{\circ}(700\,^{\circ}C) = -1025\,kJ{\cdot}mol^{-1} \quad (4)$$

$$Nd_2O_3 + Fe_2O_3 = FeNdO_3, \quad \Delta G^{\circ}(1000\,^{\circ}C) = -1091\,kJ{\cdot}mol^{-1} \quad (5)$$

Based on above observations, the overall oxidation reaction of Nd–Fe–B magnet scraps can be written as Reaction (6). It assumes that Nd_2O_3, B_2O_3 and Fe_2O_3 are the final forms of oxides in the powder mixtures.

$$Nd_2Fe_{14}B + 51/4O_2 = Nd_2O_3 + 1/2B_2O_3 + 7Fe_2O_3 \quad (6)$$

From TG curves it can be seen that the mass increase ends at around 900 °C. The final mass gain is 33.76 %. The mass gain calculated according to the chemical compositions listed in Table 1 is 34.4 %, assuming that all elements are fully oxidized. It is thus confirmed experimentally that all the elements in the powder mixtures are close to be fully oxidized.

3.2 Reduction process

3.2.1 Separation of rare earth elements and Fe

The chemical potentials of oxygen for each reaction between the elements and the corresponding oxides were calculated using the HSC Chemistry software. The calculated results are shown in Fig. 4. The rare earth elements Nd, Pr and La have very similar thermodynamic properties, so only the oxygen potential of Nd is shown. The calculated results show that Fe_2O_3 can be reduced to iron by carbon at >700 °C. B_2O_3 will be reduced by carbon at temperatures of >1650 °C. The other oxides, such as alumina and rare earth oxides, are hardly reduced by carbon in the experimental temperature range. Based on the difference of the reduction temperature, Fe_2O_3 can be reduced into metal phase and the rare earth elements remain in oxide phase.

Figure 5a shows macroimage of the oxides of Nd–Fe–B materials after roasting in a muffle furnace for 2 h at 1000 °C and Fig. 5b shows the cross section of the sample after reduced at 1550 °C for 1 h. It clearly displays that the green rare earth oxides containing slag cover the Fe-based metal phase. The oxide and the metal were further examined using microscope observations. Figure 6a shows OM image of the slag. Some Fe droplets exist in the oxide phase. Because of the difference of density between oxide and metal phase and the high viscosity of the oxide phase, it is assumed that the metal droplets gradually grow and aggregate to the bulk metal phase during the reduction process. Nevertheless, this process is time-consuming, and some Fe droplets will remain in the slag during an inadequate reaction holding time. OM image of the Fe-based metal phase, as shown in Fig. 6b, shows the typical eutectic structure of Fe metal phase, indicating that the content of carbon in the metal is at about 4.3 %.

The slag was further examined by BSE–SEM and EDS analysis, as shown in Fig. 7. The dark phase in BSE image is the metal particles, as confirmed by EDS element mappings. There are two different phases in the oxides: the grey and the white phases. The grey phase in regular shape is the rare earth oxide phase with a certain amount of alumina. The white phase containing less alumina is mainly the rare earth oxides. Table 2 lists the contents of the main elements distributed in the different phases. The content of the rare earth elements is almost equal to the content of Al in the grey phase. From the XRD pattern of the slag shown in Fig. 8, it is identified as $REAlO_3$, a peroskite phase. Alumina can hardly be reduced to metal phase in the experimental conditions, and it will go finally to $REAlO_3$ (RE = Nd, Pr, La) phase [17, 18]. Alumina will become an impurity that cannot be removed in this pyrometallurgical process. Because the rare earth oxide can

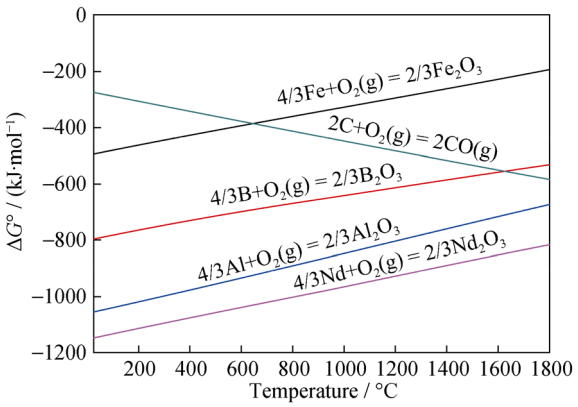

Fig. 4 Chemical potentials of oxygen in different reactions

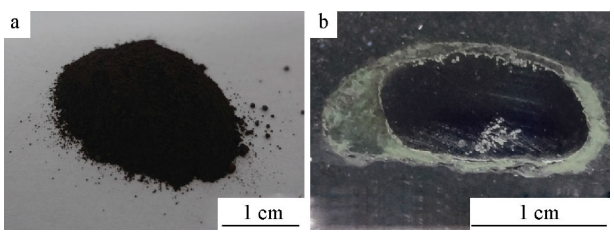

Fig. 5 Macroimages of **a** oxides of NdFeB and **b** cross section of reduced product

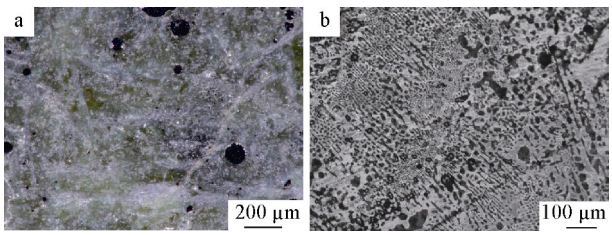

Fig. 6 OM images of **a** rare earth oxide phase and **b** metal phase

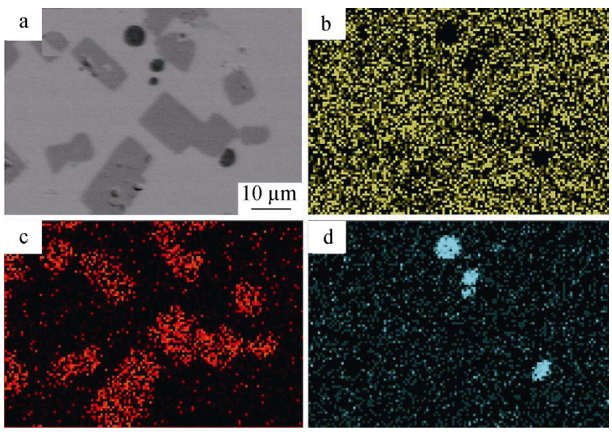

Fig. 7 BSE image of oxide phase **a** and EDS element mappings of **b** Nd, **c** Al and **d** Fe

Table 2 Contents of elements in different phases of rare earth containing slag by EDS

Elements	Dark phase		White phase		Grey phase	
	w/wt%	*x*/at%	*w*/wt%	*x*/at%	*w*/wt%	*x*/at%
Nd	*	*	61.85	25.06	76.18	54.12
Pr	*	*	10.70	4.44	14.60	10.62
La	*	*	2.97	1.25	4.19	3.09
Al	*	*	13.55	29.36	*	*
O	*	*	10.92	39.90	5.02	32.17
Fe	99.12	96.05	*	*	*	*
C	0.88	3.95	*	*	*	*

* Undetected

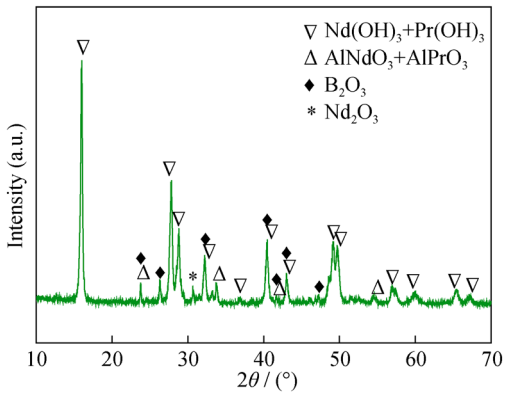

Fig. 8 XRD pattern of rare earth containing slag

easily adsorb moisture, it will gradually convert to rare earth hydroxide [19]. The rare earth hydroxide identified in Fig. 8 is considered as the result of the deliquescent effect of the rare earth oxides. In the present investigation, most of the rare earth oxides change to rare earth hydroxides after setting in the air for about 72 h.

3.2.2 Concentration of oxide phase

The concentrations of the oxide phase are displayed in Table 3 after removing Fe particles by magnetic separation. The results in Table 3 were normalized. As indicated in Fig. 4, rare earth oxides and alumina will hardly be reduced to metal phase in the current experimental conditions. The concentration of rare earth oxides and alumina shows no variation neither with the temperature of the reduction process nor with the reaction time, while Fe_2O_3 can be reduced to metal phase completely at the experimental conditions.

Boron oxide in the oxide phase decreases with the increase in treating temperature. It means that B_2O_3 can be reduced to metal phase by carbon in the experimental temperatures. The content of boron oxide in oxide phase can also be reduced with the increase in reaction time, as shown in Table 3. This rather agrees with the experimental observation by Nakamoto et al. [15]. Higher reduction temperature and long reaction time will help to extract high-purity rare earth oxides from magnet scraps. The purity of the rare earth oxides reaches 95 % at 1550 °C after holding for 7 h. Because of lack of physicochemical properties of RE_2O_3–B_2O_3–Al_2O_3 system, the optimal conditions for the high-temperature extraction process still require to be investigated in the future.

4 Conclusion

A new high-temperature pyrometallurgical process for the extraction of rare earth elements from waste Nd–Fe–B permanent magnet scraps was proposed. The process involves two steps, i.e. first oxidization of the magnet particles and then selective reduction of the oxides. Rare earth elements in $Nd_2Fe_{14}B$ powder mixture are first oxidized to rare earth oxides. Fe is then oxidized at relative higher temperatures. $FeNdO_3$ forms around 700 °C. Here, Nd also represents the other rare earth elements Pr and La for simplicity. The final oxidation product consists of Fe_2O_3, $FeNdO_3$ and a small amount of Nd_2O_3 after heating to 1000 °C for about 2 h. Iron oxides in the mixture can be easily reduced to metal phase by carbon at temperature range of 1400–1550 °C. Almost all the rare earth elements remain in oxide phase. The purity of the rare earth oxide

Table 3 Composition oxide phase under different experimental conditions

T/°C	Holding time/h	$w(Nd_2O_3)$/wt%	$w(Pr_2O_3)$/wt%	$w(La_2O_3)$/wt%	$w(Al_2O_3)$/wt%	$w(B_2O_3)$/wt%
1400	1	75.75	10.63	5.93	2.40	5.29
1500	1	76.34	10.68	5.47	2.85	4.66
1550	1	77.62	10.88	5.31	2.52	3.67
1550	3	77.16	10.95	6.14	2.45	3.30
1550	5	78.76	10.93	5.17	2.15	2.98
1550	7	79.02	11.21	5.12	2.69	1.96

can reach 95 % at 1550 °C for 7 h. Increasing reduction temperature and extending treated time help in removal of B_2O_3 in rare earth oxides.

Acknowledgments This study was financially supported by the National Key Basic Research Program of China (No. 2012CB722805).

References

[1] Sagawa M, Fujimura S, Yamamoto H, Matsuura Y, Hiraga K. Permanent magnet materials based on the rare earth–iron–boron tetragonal compounds. IEEE Trans Magn. 1984;20(5):1584.
[2] Wang RQ, Chen B, Li J, Liu Y, Zheng Q. Structural and magnetic properties of backward extruded Nd–Fe–B ring magnets made by different punch chamfer radius. Rare Met. 2014;33(3):304.
[3] Bi J, Shao S, Guan W, Wang L. State of charge estimation of Li-ion batteries in electric vehicle based on radial-basis-function neural network. Chin Phys B. 2012;21(11):118801.
[4] Itoh M, Miura K, Machida K. Novel rare earth recovery process on Nd–Fe–B magnet scrap by selective chlorination using NH_4Cl. J Alloy Compd. 2009;477(1–2):484.
[5] Asabe K, Saguchi A, Takahashi W, Suzuki RO, Ono K. Recycling of rare earth magnet scrap: part I. Carbon removal by high temperature oxidation. Mater Trans. 2001;42(12):2487.
[6] Suzuki RO, Saguchi A, Takahashi W, Yagura T, Ono K. Recycling of rare earth magnet scraps: part II. Oxygen removal by calcium. Mater Trans. 2001;42(12):2492.
[7] Li Y, Evans HE, Harris IR, Jones IP. The oxidation of NdFeB magnets. Oxid Met. 2003;59(1–2):167.
[8] Preston JS, Cole PM, Craig WM, Feather AM. The recovery of rare earth oxides from a phosphoric acid by-product: part 1. Leaching of rare earth values and recovery of a mixed rare earth oxide by solvent extraction. Hydrometallurgy. 1996;41(1):1.
[9] Xiao YF, Feng ZY, Hu GH, Huang L, Huang XW, Chen YY, Li ML. Leaching and mass transfer characteristics of elements from ion-adsorption type rare earth ore. Rare Met. 2015;34(5):357.
[10] Takeda O, Okabe TH, Umetsu Y. Phase equilibrium of the system Ag–Fe–Nd, and Nd extraction from magnet scraps using molten silver. J Alloy Compd. 2004;379(1–2):305.
[11] Okabe TH, Takeda O, Fukuda K, Umetsu Y. Direct extraction and recovery of neodymium metal from magnet. Mater Trans. 2003;44(4):798.
[12] Xu Y, Chumbley LS, Laabs FC. Liquid metal extraction of Nd from NdFeB magnet scrap. J Mater Res. 2000;15(11):2296.
[13] Takeda O, Okabe TH, Umetsu Y. Recovery of neodymium from a mixture of magnet scrap and other scrap. J Alloy Compd. 2006;408–412:387.
[14] Uda T. Recovery of rare earths from magnet sludge by $FeCl_2$. Mater Trans. 2002;43(1):55.
[15] Nakamoto M, Kubo K, Katayama Y, Tanaka T, Yamamoto T. Extraction of rare earth elements as oxides from a neodymium magnetic sludge. Metall Mater Trans B. 2011;43(3):468.
[16] Parida SC, Dash S, Singh Z, Prasad R, Jacob KT, Venugopal V. Thermodynamic studies on $NdFeO_3$. J Solid State Chem. 2002;164(1):34.
[17] Fabrichnaya O, Seifert HJ. Assessment of thermodynamic functions in the ZrO_2–Nd_2O_3–Al_2O_3 system. Calphad. 2008;32(1):142.
[18] Yamaguchi O, Sugiura K, Mitsui A, Shimizu K. New compound in the system La_2O_3–Al_2O_3. J Am Ceram Soc. 1985;68(2):44.
[19] Hamano H, Kuroda Y, Yoshikawa Y, Nagao M. Adsorption of water on Nd_2O_3: protecting a Nd_2O_3 sample from hydration through surface fluoridation. Langmuir. 2000;16(17):6961.